

Creation of X-linked Alport Syndrome Rat Model with *Col4a5* Deficiency

Masumi Namba¹, Tomoe Kobayashi^{1*}, Mayumi Kohno^{1*}, Takayuki Koyano¹, Takuo Hirose^{2,3}, Masaki Fukushima^{1,4}, Makoto Matsuyama¹.

¹ Division of Molecular Genetics, Shigei Medical Research Institute, Okayama, Japan.

² Division of Nephrology and Endocrinology, Faculty of Medicine, Tohoku Medical and Pharmaceutical University, Sendai, Japan.

³ Department of Endocrinology and Applied Medicine, Tohoku University Graduate School of Medicine, Sendai, Japan.

⁴ Shigei Medical Research Hospital, Okayama, Japan.

* These authors contributed equally to this work.

Corresponding to Makoto Matsuyama;

Division of Molecular Genetics, Shigei Medical Research Institute.

2117 Yamada, Minami-ku, Okayama 701-0202, Japan.

TEL: +81-86-282-3113

e-mail: matsuyama@shigei.or.jp

Summary

Alport syndrome is an inherited chronic human kidney disease, characterized by glomerular basement membrane abnormalities. This disease is caused by mutations in *COL4A3*, *COL4A4*, or *COL4A5* gene. The knockout mice for *Col4a3*, *Col4a4*, and *Col4a5* are developed and well characterized for the study of Alport syndrome. However, disease progression and effects of pharmacological therapy depend on the genetic variability. This model is reliable only to mice. Therefore in this study, we created a novel Alport syndrome rat model utilizing rGONAD technology. *Col4a5* deficient rats showed hematuria, proteinuria, high levels of BUN, Cre, and then died at 18 to 28 weeks of age (Hemizygous mutant males). Histological and ultrastructural analyses displayed the abnormalities including parietal cell hyperplasia, mesangial sclerosis, and interstitial fibrosis. Then, we demonstrated that $\alpha3/\alpha4/\alpha5$ (IV) and $\alpha5/\alpha5/\alpha6$ (IV) chains of type IV collagen disrupted in the *Col4a5* deficient rats. Moreover, immunofluorescence analyses revealed that some glomeruli of *Col4a5* mutant rats were found to be disrupted from postnatal day 0. Thus, *Col4a5* mutant rat is a reliable candidate for Alport syndrome model for underlying the mechanism of renal diseases and further identifying potential therapeutic targets for human renal diseases.

Introduction

Type IV collagen networks are the structural foundation for all basement membranes, consist of 6 different chains from COL4A1 to COL4A6 in mammals.^{1, 2} The 6 chains assemble into 3 types of heterotrimers (protomers), which have distinct tissue distribution and function. In the mammalian kidney, the glomerular basement membrane (GBM), requiring long-term maintenance of the glomerular filtration functions, is composed of $\alpha 3/\alpha 4/\alpha 5$ (IV) isoforms. Whereas $\alpha 1/\alpha 1/\alpha 2$ (IV) isoforms are found in all basement membranes, and $\alpha 5/\alpha 5/\alpha 6$ (IV) isoforms are detected in Bowman's capsule (BC).

Alport syndrome is a basement membrane disorder, characterized by hereditary nephropathy that results in irreversible, progressive renal failure.³ Alport syndrome is caused by mutations in *COL4A3*, *COL4A4*, or *COL4A5* gene encoding type IV collagen $\alpha 3$, $\alpha 4$, or $\alpha 5$ chains.⁴ Defects in the *COL4A5* gene cause X-linked Alport syndrome, which accounts for about 80% of Alport syndrome.⁵ And the remaining cases are associated with mutations in *COL4A3* or *COL4A4* genes. The pathological events of Alport syndrome are very similar, are found that lack of *COL4A3*, *COL4A4*, or *COL4A5* resulted in the degradation of $\alpha 3/\alpha 4/\alpha 5$ (IV) heterotrimers.¹

In the past decades, several Alport syndrome animal models have been

produced in mice. The knockout mice for *Col4a3*, *Col4a4*, and *Col4a5* are developed and well characterized.⁶⁻⁹ Moreover, there are several Knock-out and Knock-in mice harboring missense, nonsense, deletion mutant of *Col4a5*.^{10, 11} These model mice led important aspects of the renal disease. Whereas, there are some significant differences depend on genetic background in Alport syndrome model mice.^{8, 12, 13} For example, 129X1/Sv or C57BL/6 was different patterns of disease progression in *Col4a3*^{-/-} mice.¹⁴ Indeed, in the human patients, the disease progression and effects of pharmacological therapy were shown to genetic variability. However, in spite of variabilities displayed in the genetic background, only a few mammal models (only mice and dogs) have been established for Alport syndrome.

The laboratory rat (*Rattus norvegicus*) is a common experimental model for the human diseases and the drug testing.¹⁵⁻¹⁷ For example, Wistar Kyoto (WKY) rat strain is known to be uniquely susceptible to crescentic glomerulonephritis among the strains tested.¹⁸⁻²¹ Although there are several advantages comparing with mice, production of genetically engineered rat models has not yet been extensively proceeded during the past decades. The recent CRISPR/Cas9 system is the simplest for generating rats carrying a modified genome,^{22, 23} however, the standard method for genome-editing in mammals involves 3 major steps: isolation of zygotes from females,

micromanipulation *ex vivo*, and transfer into pseudopregnant females. These 3 steps require extremely high level of technical expertise and its proficiency of the researchers as well as technicians. To simplify these complexed and laborious processes, we developed more simple and reliable method for genome editing in mice and rats are now available, namely *i*-GONAD and rGONAD (rat Genome-editing via Oviductal Nucleic Acids Delivery).²⁴⁻²⁷ The rGONAD method involves 2 key steps: an injection of the solution containing Cas9 protein, guide RNA and single strand DNA (ssDNA) into the oviduct, followed by electroporation. The rats that have undergone rGONAD are bred in routine way until birth. Moreover, rGONAD is highly efficient in both knock-out and knock-in rats.²⁶

In the present study, we attempted to create Alport syndrome rat model using rGONAD technology. We developed *Col4a5* deficient mutant rats, identical to the *Col4a5* G5X mutant mice,⁹ which showed progressive glomerular disease and CKD phenotypes with renal fibrosis. And we investigated whether the mutant rats were applicable for the Alport syndrome model.

Results

Generation of *Col4a5* deficient rats by the rGONAD method

On the basis of human mutations as described previously, we introduced novel *Col4a5* deficient rats with CRISPR/Cas9 and rGONAD technology.²⁶ Tandem STOP codons were integrated into 27 bases after the first ATG in rat *Col4a5* gene (Supplemental Figure 1A). The mutation was verified by PCR followed by DNA sequencing, resulting to be expressed only 9 amino acids of COL4A5 at its N-terminus (Supplemental Figure 1B, C). We detected no COL4A5 protein expression in the *Col4a5* deficient male rats by immunofluorescence and Western blot analyses with monoclonal antibodies against the NC1 (C-terminus) domains of type IV collagens (See below; Figure 5, 6). In addition, the mutant rats which were integrated the other frame-shift tandem STOP codons (*Col4a5* 15aa stop; Supplemental Figure 2) and were deleted 56bp including the first ATG (*Col4a5* 56bp deletion; Supplemental Figure 3), also generated, and revealed the same phenotype as Alport syndrome rats (Supplemental Figure 2, 3). These data collectively indicate the successful generation of *Col4a5* deficient rats.

Physiological analyses in *Col4a5* mutants

Col4a5 deficient rats were viable, fertile, and expected Mendelian ratios.

However, all hemizygous mutant males died from 18 to 28 weeks of age (n=58; Figure 1A). Heterozygous mutant females died at 35 to 100 weeks of age, among them, approximately 30 % of females survived over 100 weeks (n=33, Figure 1A). To assess of functional and histological abnormalities of the kidney, we measured the hematuria and proteinuria in *Col4a5* deficient rats. Hematuria was found from postnatal 21 days in hemizygous mutant males, and from 4 weeks of age in heterozygous mutant females (data not shown). Proteinuria was observed (about 6.0 mg/16 hours) by 6 weeks of age in hemizygous mutant males (see Supplemental Table 1), then, increased > 20.0 mg/16 hours in all of mutant males after 12 weeks of age (n=35), and 62% of mutant females in 16 week of age (n=28/45) (Figure 1B). On the contrary, these phenomena were not detected in wildtype male and female rats in any week of age (Figure 1B).

Mutant males showed decrease of body weight and increase of urine volume, compared with those of wildtype males (Figure 1C, D). The levels of blood urea nitrogen (BUN) and serum creatinine (Cre) in serum highly increased in 20 weeks of age of mutant males (Figure 1E, F).

Renal histology in *Col4a5* deficient rats

The kidney sections from wildtype and *Col4a5* deficient rats were stained with hematoxylin and eosin (HE), Periodic acid Schiff (PAS), periodic acid methenamine silver (PAM), and Masson trichrome (MT) (Figure 2). At 8 weeks of age, the glomeruli exhibited capillary tuft collapse in hemizygous mutant males (Figure 2A). However, the kidney displayed overall sparing of the tubulointerstitium (Figure 2A). By the 20 weeks of age in hemizygous mutant males, substantial numbers of glomeruli revealed the abnormalities, including parietal cell hyperplasia mimicking crescent formation, focal sclerosis, and with overall sparing of the tubulointerstitium (Figure 2B, Supplemental Figure 4). The kidney sections from heterozygous mutant females at 8-20 weeks of age displayed focal abnormalities of the glomeruli and tubulointerstitium (Figure 2A, B, Supplemental Figure 4).

The 3 dimensional ultrastructure of GBM observed by low-vacuum scanning electron microscopy (LVSEM) revealed the coarse meshwork structure of GBM with numerous pin-holes in hemizygous mutant males, in contrast to the smoothly arranged surface in the wildtype males (Figure 3, Supplemental Figure 5).

Renal glomerular and tubulointerstitial fibrosis in *Col4a5* deficient rats

To evaluate the fibrosis of glomeruli and tubulointerstitium in *Col4a5* deficient rats, we examined the kidney sections from wildtype and *Col4a5* deficient rats stained with antibodies specific for α -smooth muscle actin (α -SMA) and fibronectin (Figure 4). Immunostaining showed expression level of α -SMA, a marker of renal glomerular and tubulointerstitial fibrosis, was increased around the glomeruli in the kidneys from hemizygous mutant males when compared with those of wildtype littermates at 20 weeks of age, but was not detected in the renal tubular epithelia (Figure 4A). The kidney sections from the heterozygous females were rarely detected by 20 weeks of age (Figure 4A, Supplemental Figure 6). In contrast, the expression level of fibronectin, a marker of pathological deposition of extracellular matrix (ECM), was increased in 12 weeks of age of the hemizygous mutant males (Figure 4B). We then observed fibronectin expression in the heterozygous mutant females at 12 weeks of age (Figure 4B, Supplemental Figure 7). These results suggest that the increase of fibronectin expression might represent the mesangial sclerosis and interstitial fibrosis in *Col4a5* deficient males and females.

.

The expression of type IV Collagen α 1-6 in *Col4a5* deficient rats

The type IV collagen networks comprised of $\alpha 1/\alpha 1/\alpha 2$ (IV) (all basement membranes), $\alpha 3/\alpha 4/\alpha 5$ (IV) (GBM), and $\alpha 5/\alpha 5/\alpha 6$ (IV) (Bowman's capsule) protomers were observed in the glomeruli. To examine whether localizations and/or the levels of the proteins were changed in the *Col4a5* deficient rats, we investigated *Col4a5* deficient rats with graded levels of the other's type IV collagen $\alpha 1$, $\alpha 2$, $\alpha 3$, $\alpha 4$, and $\alpha 6$ (IV). First, we produced novel monoclonal antibodies that specifically recognize rat COL4A6 protein. We obtained rCol4A6 antibodies by injecting the antigen in *Col4a5* deficient males, but we could not obtain the specific antibody injected to wildtype rats at all. Immunoblot analysis revealed that the monoclonal anti-rCOL4A6, reacted specifically with a band corresponding to the position of the similar molecular weights in recombinant rCOL4A6 proteins, and only reacted with rCOL4A6, but not with other rCOL4 proteins (Supplemental Figure 8).

To determine whether localization of type IV collagens of $\alpha 1-6$ (IV) in the kidney of *Col4a5* deficient rats changed, we performed the immunofluorescence analyses. At 8-20 weeks of age, COL4A5 expression was absent in the hemizygous mutant males, and present in a mosaic pattern in heterozygous mutant females (Figure 5A, B, Supplemental Figure 9-12). The expressions of COL4A3, COL4A4, and COL4A6 were also absent in *Col4a5* deficient males, and present in a mosaic pattern in

heterozygous mutant females (Figure 5A, B, Supplemental Figure 9-12). At 8 weeks of age, in contrast, expressions of COL4A1 and COL4A2 were present in *Col4a5* deficient rats (Figure 5A, Supplemental Figure 9). At 20 weeks of age, the kidney showed a strong accumulation of COL4A1 and COL4A2 proteins in both GBM and Bowman's capsule (Figure 5B, Supplemental Figure 9-12). These data suggest that $\alpha3/\alpha4/\alpha5$ (IV) and $\alpha5/\alpha5/\alpha6$ (IV) chains of type IV collagen disrupted in the *Col4a5* deficient rats.

To verify the results of the immunostaining, we analyzed protein expressions noncollagenous domains 1 (NC1) that were prepared from kidneys of wildtype and hemizygous mutant males by Western blot analyses (Figure 6). There were no bands detectable NC1 domains of type IV Collagen $\alpha3$, $\alpha4$, and $\alpha5$ (IV), derived from $\alpha3/\alpha4/\alpha5$ (IV) complexes, in kidney of *Col4a5* deficient males (Figure 6). Then, the NC1 domains of type IV Collagen $\alpha5$ and $\alpha6$ (IV), derived from $\alpha5/\alpha5/\alpha6$ (IV) complexes, were also absent, whereas the blotting for the NC1 domains of type IV Collagen $\alpha1$ and $\alpha2$ (IV), derived from $\alpha1/\alpha1/\alpha2$ (IV) complexes, were present in the hemizygous mutant males as well as wild type (Figure 6). Therefore, these findings fully corroborate the results of immunofluorescence analyses.

***Col4a5* deficient rats in early renal developmental stage**

Alport syndrome has well been studied in terms of adult renal pathogenesis, although little is still known in the early development. We focused to investigate early renal pathology with the *Col4a5* deficient rats. To determine when COL4A5 protein expresses in the postnatal kidney, we performed immunostaining on wildtype and on *Col4a5* deficient males from birth to 28 days of age (Figure 7A). After birth (P0), COL4A5 was expressed in only GBM in wildtype rats (Figure 7A). During postnatal day (P7), this expression was spread to Bowman's capsule and basement membrane of ureter epithelial cells (Figure 7A). There were no COL4a5 staining detectable in the *Col4a5* mutant male kidneys with anti-COL4A5 antibody (Figure 7A).

To detect renal failure in postnatal stage, we examined expression of nestin, nephrin, and synaptopodin in *Col4a5* hemizygous males. Immunofluorescence analyses showed nestin, a marker of intermediate filament protein, was located orderly in glomeruli of wildtype kidneys after birth (Figure 7A). In contrast, the expression of some glomeruli was found to be disrupted from postnatal day 0 (Figure 7A). Immunofluorescence analyses also revealed that expression of nephrin, a marker of transmembrane cell adhesion molecule, was found to locate at slit diaphragm in GBM, and synaptopodin, a marker of slit diaphragm proteins expressed in GBM, were disorganized, and found aggregated (Figure 7B). Thus, these observations certainly

suggest that slit diaphragm in GBM was already disrupted at the postnatal development of the *Col4a5* deficient kidneys.

Discussion

The present study showed that we successfully created a novel Alport syndrome rat model with rGONAD technology. *Col4a5* deficient rats revealed typical physiological, pathological, and also histological characteristics of Alport syndrome. Furthermore, it will be especially useful for studying progress of occurrence of the renal diseases of Alport syndrome beginning from postnatal stages.

Occurrence of Alport syndrome is caused by mutations in *COL4A3*, *COL4A4*, or *COL4A5*.⁴ Several mouse models in *Col4a3*, *Col4a4*, and *Col4a5* mutation have been known and characterized.^{6-10, 13} *Col4a3*^{-/-} or *Col4a4*^{-/-} mice are well used for studying treatments of Alport syndrome compared to *Col4a5*^{-Y} mice.²⁸⁻³¹ Because, a survival ratio of *Col4a5*^{-Y} mice was so diffusive ranged from 6 to 34 weeks,⁹ in contrast, those of *Col4a3*^{-/-} or *Col4a4*^{-/-} mice were more uniform (from 13 to 26 weeks).^{32, 33} In this study, *Col4a5* mutant males died at 18 to 28 weeks (about 95 % from 20 to 26 weeks) of age. Thus, it is useful to study experiments for prolong the lifespan of *Col4a5* deficient rats for effects of the drug, food, and other factors.

In the present study, we were able to produce *Col4a5* mutant rats of WKY strain. Some number of glomeruli exhibited capillary tuft collapse at 8 weeks of age, and more glomeruli revealed abnormalities with crescent formation and focal sclerosis

at the 20 weeks of age in *Col4a5* mutant males. The levels of BUN and Cre in serum highly increased in 20 weeks of age, and then died at around 24 weeks of age in hemizygous mutant males. These physiological and pathological features correspond to those of previously reported *Col4a3*^{-/-} with C57BL/6 mouse strain.^{12, 14} However, *Col4a3*^{-/-} with 129X1/Sv mouse strains showed much earlier progression of disease, died at around 12 weeks of age.^{12, 32, 34} Therefore, comparison of a survival ratio between different strains of mice and rats should be carefully studied them, and further studies are required to draw a definite conclusion. In further study, other rat strains of *Col4a5* mutant using rGONAD method can be expected.

The laboratory rat has long been recognized as a preferred experimental animal in wide areas of biomedical science.^{22, 35} In some situation, rat is considered as a more relevant model among mammals. For example, physiology of rat is greatly well documented, because its larger body size affords the opportunity for serial blood draw studies. In particular, blood pressure measurement by telemetry is easier to perform and more reliable in rats compared to smaller mice.^{36, 37} Moreover, there are several rat strains in order to perform specific studies, i.e, SHR for hypertension.³⁸ Although genome engineering experiments of rat have yet not been extensively proceeded, it is readily applicable to produce the gene-editing mutant rats in *Col4a5* gene of the strains

by rGONAD method. The model rats might provide new insight into the study of the relationship between renal disease such as Alport syndrome and other blood pressure related diseases.

In conclusion, we have described creation of a novel rat model of Alport syndrome. This rat model should be available for the study of progressive renal failure having basement membrane abnormality after birth. Thus, *Col4a5* mutant rat is a reliable candidate for Alport syndrome model animal for underlying the mechanism of renal diseases and further identifying potential therapeutic targets for human renal diseases.

Materials and Methods

Animals

WKY/NCrl rats were obtained from Charles River. The rats were kept with a 12:12-h light: dark cycle. They were given free access to drinking water and food. All animals were handled in strict accordance with good animal practice as defined by the relevant national and/or local animal welfare bodies, and all animal works were approved by the appropriate committee (permission number: #17006).

Generation of type IV Collagen $\alpha 5$ KO rats

Type IV Collagen $\alpha 5$ deficient rats were produced by the rGONAD method as previously described.²⁶ Briefly, gene targeting strategy is designed to integrate tandem STOP codons into 27 bases after the first ATG in rat *Col4 $\alpha 5$* gene (Supplemental figure S1A). Guide RNAs were designed using CHOPCHOP (<https://chopchop.cbu.uib.no/>) (Supplemental figure S1A).

For the preparation of CRISPR/Cas9 reagents, Alt-RTM CRISPR-Cas9 system (Integrated DNA Technologies [IDT, Coralville, IA]) was used in accordance with the manufacturer's protocol. Approximately 2-2.5 μ l of electroporation solution was injected into the rat oviductal lumen from up-stream of ampulla using a micropipette. The

electroporation was performed using a NEPA21 (NEPA GENE Co. Ltd., Chiba, Japan).

Genotyping

Gene alteration was certified by PCR followed by DNA sequencing, as described previously.³⁹ Rat genomic DNA was isolated from ear-piece or tail. Genotyping was performed by PCR with the following primers (see also Supplemental figure S1A):

rCol4a5-fw, (5'-GCTCTCTTCCCAATAACCCCT-3'), rCol4a5-rv,
(5'-CAATTTTGACTTCCCTGGCCA-3').

Urine and blood parameters

Urine samples were collected for 16 hours by placed rats in metabolic cages individually, every 4 weeks over 52 weeks (see Supplemental Table 1). Proteinuria level was measured by a modified method using 3 % sulfosalicylic acid. Blood samples (n=6 each) were collected from the tail and centrifuged at 3000 g for 5min to obtain blood serum. Blood urea nitrogen (BUN) of serum was measured using Colorimetric Detection Kit (Arbor Assays, Michigan, USA). Serum Creatinine (Cre) levels were measured Jaffe's method (FUJIFILM Wako Pure Chemical Corporation, Osaka, Japan). All measurements were carried out according to manufacturer's recommended

protocols.

Histological analyses

Rat kidneys were soaked in 10% buffered neutral formalin at least overnight, and embedded in paraffin after dehydrated. The embedded kidneys were sliced 1-2 μm thickness. These slides were stained with hematoxylin and eosin (HE), periodic acid Schiff (PAS), periodic acid methenamine silver (PAM) and masson's trichrome (MT) by standard methods.

Low vacuum scanning electron microscopy (LVSEM)

Under LVSEM, 3 dimensional ultrastructure of GBMs of Alport syndrome, the kidney was examined as described previously.⁴⁰ In brief, renal paraffin sections of 4 μm thickness were stained with PAM. The sections on the slides were directly observed without a cover clip, with LVSEM (Hitachi TM4000; Hitachi Co. Ltd., Tokyo, Japan) at acceleration voltage of 15 kV with 30Pa.

Preparation of Recombinant Proteins

His-tagged (for production of antibody) and MBP-tagged (for immunoblotting) NC1

domains of type IV Collagen α 1-6 (V) were expressed in BL21-CodonPlus-RP (Agilent Technologies, Santa Clara, CA) transformed with pET-28a (Invitrogen) and pMAL (New England Biolabs, Beverly, MA), respectively. Each His or MBP fusion protein was purified through affinity chromatography with TALON metal affinity resin (Clontech, Palo Alto, CA) or with amylose resin (New England Biolabs), respectively.

Antibody

We produced rat monoclonal rCOL4A6, as described previously.^{41, 42} Briefly, the antigen emulsion was injected to *Col4a5* deficient males. The treated rats were sacrificed 21 days after the injection, and the lymphocytes were fused with SP2/0-Ag14 myeloma cells. After the cell fusion, culture supernatants were screened to confirm positive clones by solid-phase enzyme-linked immunosorbent assay (ELISA).

The following primary antibodies were used: rat monoclonal type IV collagen α 1(IV) (H11), α 2 (IV) (H22), α 3 (IV) (H31), α 4 (IV) (H43), α 5(IV) (H52), (In our institute),⁴³ SMA (1A4, Cell Signaling Technology, Beverly, MA); Fibronectin (ab6328, Abcam, Cambridge, UK); Nephrin (GP-N2, Progen, Germany); Nestin (66259-1-Ig); Synaptopodin (21064-1-AP, proteintech, Illinois), and MBP (New England Biolab) Primary antibodies were detected using species-specific secondary antibodies

conjugated to either Alexa Fluor 488 or 555 (Molecular probes).

Tissue extract preparation and immunoblotting-

Rat kidneys were homogenized and incubated at 37°C for 4 hours with 1mg kidney lysates and 200 µg (1000 U) of collagenase (Brightase-C; Nippi, Okayama, Japan) in digestion buffer (20 mM HEPES, 10 mM CaCl₂) with protease inhibitor cocktail (Nacalai, Kyoto, Japan). Protein concentrations for cell extracts were determined by the Coomassie Brilliant Blue staining by SDS-PAGE gels. The lysates were loaded, transferred, and subjected to Western blotting with specific antibodies as described previously.⁴⁴

Immunofluorescence

Immunofluorescence analyses were examined, as described previously.⁴⁵ Briefly, rat kidneys were immersed in OCT compound, and snap-frozen in liquid nitrogen vapor. Subsequently, kidneys were sliced 5 µm cryostat sections and placed on slides. After dehydration by acetone, blocked in 5 % (v/v) donkey serum for 30 min at room temperature. Sections were then incubated with primary antibodies overnight at 4 °C followed by PBS wash and incubated with appropriate secondary antibodies for 1h at room temperature. DNA was also stained with 1 µg/ml DAPI. Fluorescence images

were obtained by confocal microscopy (FV1200, Olympus, Japan).

Abbreviations:

GONAD: Oviductal Nucleic Acids Delivery, *i*-GONAD: improved GONAD, rGONAD: Rat improved GONAD, WKY: Wistar Kyoto, CRISPR: Clustered Regularly Interspaced Short Palindromic Repeats, Cas: CRISPR-associated, GBM: glomerular basement membrane, BC: Bowman's capsule, ssDNA: single strand DNA, BUN: blood urea nitrogen, Cre: serum creatinine, HE: hematoxylin and eosin, PAS: Periodic acid Schiff, PAM: periodic acid methenamine silver, MT: Masson trichrome, LVSEM: low-vacuum scanning electron microscopy, ECM: extracellular matrix, NC1: noncollagenous domains 1,

Ethics approval and consent to participate

All animals were handled in strict accordance with good animal practice as defined by the relevant national and/or local animal welfare bodies, and all animal works were approved by the appropriate committee.

Competing interests

The authors declare they have no competing interests.

Funding

This work was supported in part by the Ryobi Teien Memory Foundation and Wesco Scientific Promotion Foundation.

Authors' contributions

MN, TK, MK, TK, MF, and MM conceived and designed the experiments, MN, TK, MK, TK, TH, and MM performed experiments, MN and MM wrote the manuscript. All authors read and approved the final manuscript.

Acknowledgements

We are grateful to Chieko Takahashi for animal breeding, Dr. Yoshikazu Sado for technical assistance, and Dr. Tohru Okigaki for critical comments on the manuscript. We would like to thank Dr. Fumihiro Shigei, Chairman of the Board, for financial support and continuous encouragements. This work was also supported in part by the Ryobi Teien Memory Foundation and Wesco Scientific Promotion Foundation.

Figure legends

Figure 1. **Physiological analyses in *Col4a5* mutant rats**

(A) Estimated survival functions in wildtype (WT) and *Col4a5* mutant (Hemi; hemizygous males, het; heterozygous females) rats. (B) Proteinuria in wildtype and *Col4a5* deficient rats from 4 to 52 weeks of age. (C-F) Measurements of body weight (C), urine volume (D), blood urea nitrogen (BUN) of serum (E), and serum Creatinine (Cre) in wildtype and *Col4a5* mutant males from 4 to 20 weeks of age.

Figure 2. **Histological analyses of the *Col4a5* deficient kidneys**

Representative microscopic images in wildtype (WT) and *Col4a5* mutant (Hemi; hemizygous males, Het; heterozygous females) rats at 8 weeks (A) and 20 weeks (B) of age. These tissue sections were prepared and stained with hematoxylin and eosin (HE), Periodic acid Schiff (PAS), periodic acid methenamine silver (PAM), and Masson trichrome (MT). *Scale bars*, 100 μ m.

Figure 3. **Electron photomicrographs of glomerular basement membranes in *Col4a5* mutant rats**

Representative Low-vacuum scanning electron microscopy (LVSEM) images in

wildtype (WT) and *Col4a5* mutant (Hemi) males at 8 weeks (A) and 20 weeks (B) of age. Arrowheads indicate the coarse meshwork structure of the GBMs. Arrows also indicate cut side of the capillary walls. Red insets are revealed the higher magnification of left panels. E: Endothelial cells, M: Mesangial cells, P: Podocytes, R: Red blood cells. *Scale bars*, 5 μm (left), 1 μm (right).

Figure 4. Renal fibrosis in *Col4a5* deficient rats

(A, B) Immunostaining of kidney sections with αSMA (A) or fibronectin (B) (red), nestin (green; glomeruli), and DAPI (blue; nuclei) in wildtype (WT) and *Col4a5* mutant (Hemi; hemizygous males, Het; heterozygous females) rats from 8 to 20 weeks of age. *Scale bars*, 50 μm .

Figure 5. Type IV collagen distributions in the *Col4a5* deficient kidneys

(A, B) Immunofluorescence analyses of kidney sections with antibodies against $\alpha 1-6$ (IV) (red), nestin (green; glomeruli), and DAPI (blue; nuclei) in wildtype (WT) and *Col4a5* mutant (Hemi; hemizygous males, Het; heterozygous females) rats at 8 weeks (A) and 20 weeks (B) of age. *Scale bars*, 50 μm .

Figure 6. Western blot analyses of type IV collagen in the *Col4a5* mutant kidneys

Collagenase-solubilized renal basement membranes from wildtype (W) and *Col4a5* mutant (H) males at 8 weeks of age were separated by SDS-PAGE and blotted with antibodies that specifically recognized $\alpha 1-6$ (IV) NC1 domains. D: NC1 dimer, M: NC1 monomer.

Figure 7. Early renal pathology with *Col4a5* deficient rats.

(A, B) Immunofluorescence analyses of the rat kidney sections with antibodies against (A): $\alpha 5$ (IV) (red), nestin (green; glomeruli), and DAPI (blue; nuclei), (B): Synaptopodin (red), nephrin (green), and DAPI (blue; nuclei), in wildtype (WT) and *Col4a5* mutant (Hemi) male rats after birth, postnatal (P) 7, 14, and 28 days of age.

Scale bars, 50 μ m.

Supplementary Information

Contents:

Supplemental Figure 1. Production of *Col4a5* mutant rats

Supplemental Figure 2. Analyses of “*Col4a* 15aa stop” mutant rats

Supplemental Figure 3. Analyses of “*Col4a5* 56bp deletion” mutant rats

Supplemental Figure 4. Histological analyses of the *Col4a5* deficient kidneys

Supplemental Figure 5. Electron photomicrographs of glomerular basement membranes in *Col4a5* mutant rats

Supplemental Figure 6. Renal fibrosis in *Col4a5* deficient rats

Supplemental Figure 7. Renal fibrosis in *Col4a5* deficient rats

Supplemental Figure 8. Characterization of an antibody specifically recognized type IV collagen

Supplemental Figure 9. Type IV collagen distributions in the *Col4a5* deficient kidneys at 8 weeks of age

Supplemental Figure 10. Type IV collagen distributions in the *Col4a5* deficient kidneys at 12 weeks of age

Supplemental Figure 11. Type IV collagen distributions in the *Col4a5* deficient kidneys at 16 weeks of age

Supplemental Figure 12. Type IV collagen distributions in the *Col4a5* deficient kidneys at 20 weeks of age

Supplemental Table 1. Proteinuria in *Col4a5* deficient rats

References

1. Cosgrove D, Liu S: Collagen IV diseases: A focus on the glomerular basement membrane in Alport syndrome. *Matrix Biol*, 57–58: 45–54, 2017 10.1016/j.matbio.2016.08.005
2. Fidler AL, Boudko SP, Rokas A, Hudson BG: The triple helix of collagens – an ancient protein structure that enabled animal multicellularity and tissue evolution. *J Cell Sci*, 131, 2018 10.1242/jcs.203950
3. Kruegel J, Rubel D, Gross O: Alport syndrome—insights from basic and clinical research. *Nat Rev Nephrol*, 9: 170–178, 2013 10.1038/nrneph.2012.259
4. Kashtan CE, Ding J, Garosi G, Heidet L, Massella L, Nakanishi K, et al.: Alport syndrome: a unified classification of genetic disorders of collagen IV alpha345: a position paper of the Alport Syndrome Classification Working Group. *Kidney Int*, 93: 1045–1051, 2018 10.1016/j.kint.2017.12.018
5. Bekheirnia MR, Reed B, Gregory MC, McFann K, Shamshirsaz AA, Masoumi A, et al.: Genotype–phenotype correlation in X-linked Alport syndrome. *J Am Soc Nephrol*, 21: 876–883, 2010 10.1681/ASN.2009070784
6. Cosgrove D, Meehan DT, Grunkemeyer JA, Kornak JM, Sayers R, Hunter WJ, et al.: Collagen COL4A3 knockout: a mouse model for autosomal Alport syndrome. *Genes Dev*, 10: 2981–2992, 1996 10.1101/gad.10.23.2981
7. Miner JH, Sanes JR: Molecular and functional defects in kidneys of mice lacking collagen alpha 3(IV): implications for Alport syndrome. *J Cell Biol*, 135: 1403–1413, 1996 10.1083/jcb.135.5.1403
8. Korstanje R, Caputo CR, Doty RA, Cook SA, Bronson RT, Davisson MT, et al.: A mouse Col4a4 mutation causing Alport glomerulosclerosis with abnormal collagen alpha3alpha4alpha5(IV) trimers. *Kidney Int*, 85: 1461–1468, 2014 10.1038/ki.2013.493
9. Rheault MN, Kren SM, Thielen BK, Mesa HA, Crosson JT, Thomas W, et al.: Mouse model of X-linked Alport syndrome. *J Am Soc Nephrol*, 15: 1466–1474, 2004 10.1097/01.asn.0000130562.90255.8f
10. Hashikami K, Asahina M, Nozu K, Iijima K, Nagata M, Takeyama M: Establishment of X-linked Alport syndrome model mice with a Col4a5 R471X mutation. *Biochem Biophys Res*, 17: 81–86, 2019 10.1016/j.bbrep.2018.12.003
11. Song JY, Saga N, Kawanishi K, Hashikami K, Takeyama M, Nagata M:

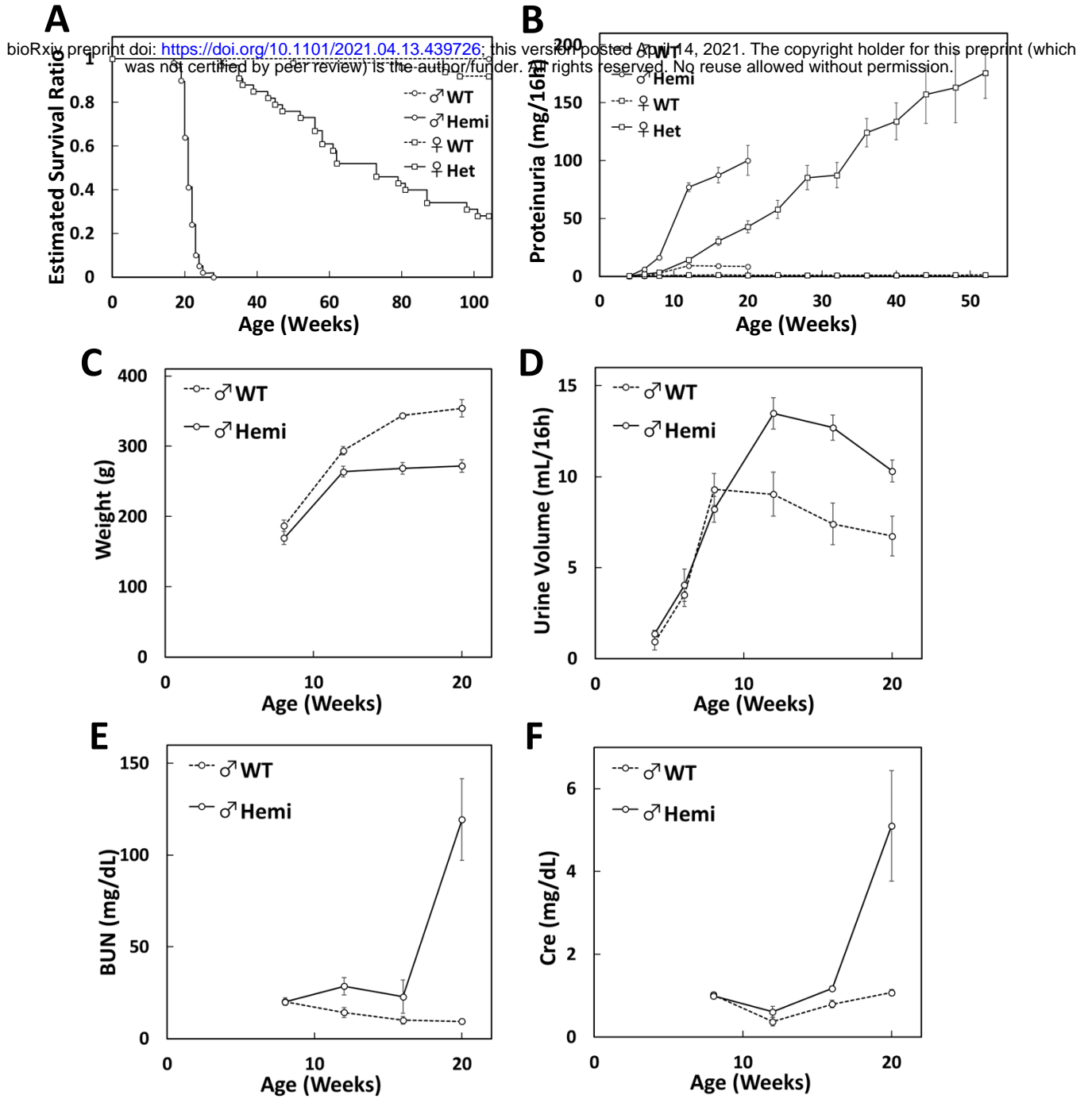
- Bidirectional, non-necrotizing glomerular crescents are the critical pathology in X-linked Alport syndrome mouse model harboring nonsense mutation of human COL4A5. *Sci Rep*, 10: 18891, 2020 10.1038/s41598-020-76068-4
12. Murata T, Katayama K, Oohashi T, Jahnukainen T, Yonezawa T, Sado Y, et al.: COL4A6 is dispensable for autosomal recessive Alport syndrome. *Sci Rep*, 6: 29450, 2016 10.1038/srep29450
 13. Falcone S, Wisby L, Nicol T, Blease A, Starbuck B, Parker A, et al.: Modification of an aggressive model of Alport Syndrome reveals early differences in disease pathogenesis due to genetic background. *Sci Rep*, 9: 20398, 2019 10.1038/s41598-019-56837-6
 14. Kang JS, Wang XP, Miner JH, Morello R, Sado Y, Abrahamson DR, et al.: Loss of alpha3/alpha4(IV) collagen from the glomerular basement membrane induces a strain-dependent isoform switch to alpha5alpha6(IV) collagen associated with longer renal survival in Col4a3^{-/-} Alport mice. *J Am Soc Nephrol*, 17: 1962-1969, 2006 10.1681/ASN.2006020165
 15. Atanur SS, Diaz AG, Maratou K, Sarkis A, Rotival M, Game L, et al.: Genome sequencing reveals loci under artificial selection that underlie disease phenotypes in the laboratory rat. *Cell*, 154: 691-703, 2013 10.1016/j.cell.2013.06.040
S0092-8674(13)00779-4 [pii]
 16. Mullins LJ, Conway BR, Menzies RI, Denby L, Mullins JJ: Renal disease pathophysiology and treatment: contributions from the rat. *Dis Model Mech*, 9: 1419-1433, 2016 9/12/1419 [pii]
10.1242/dmm.027276
 17. Yoshimi K, Mashimo T: Application of genome editing technologies in rats for human disease models. *J Hum Genet*, 2017 10.1038/s10038-017-0346-2
10.1038/s10038-017-0346-2 [pii]
 18. Sado Y, Naito I, Akita M, Okigaki T: Strain specific responses of inbred rats on the severity of experimental autoimmune glomerulonephritis. *J Clin Lab Immunol*, 19: 193-199, 1986
 19. Sado Y, Kagawa M, Rauf S, Naito I, Moritoh C, Okigaki T: Isologous monoclonal antibodies can induce anti-GBM glomerulonephritis in rats. *J Pathol*, 168: 221-227, 1992 10.1002/path.1711680211

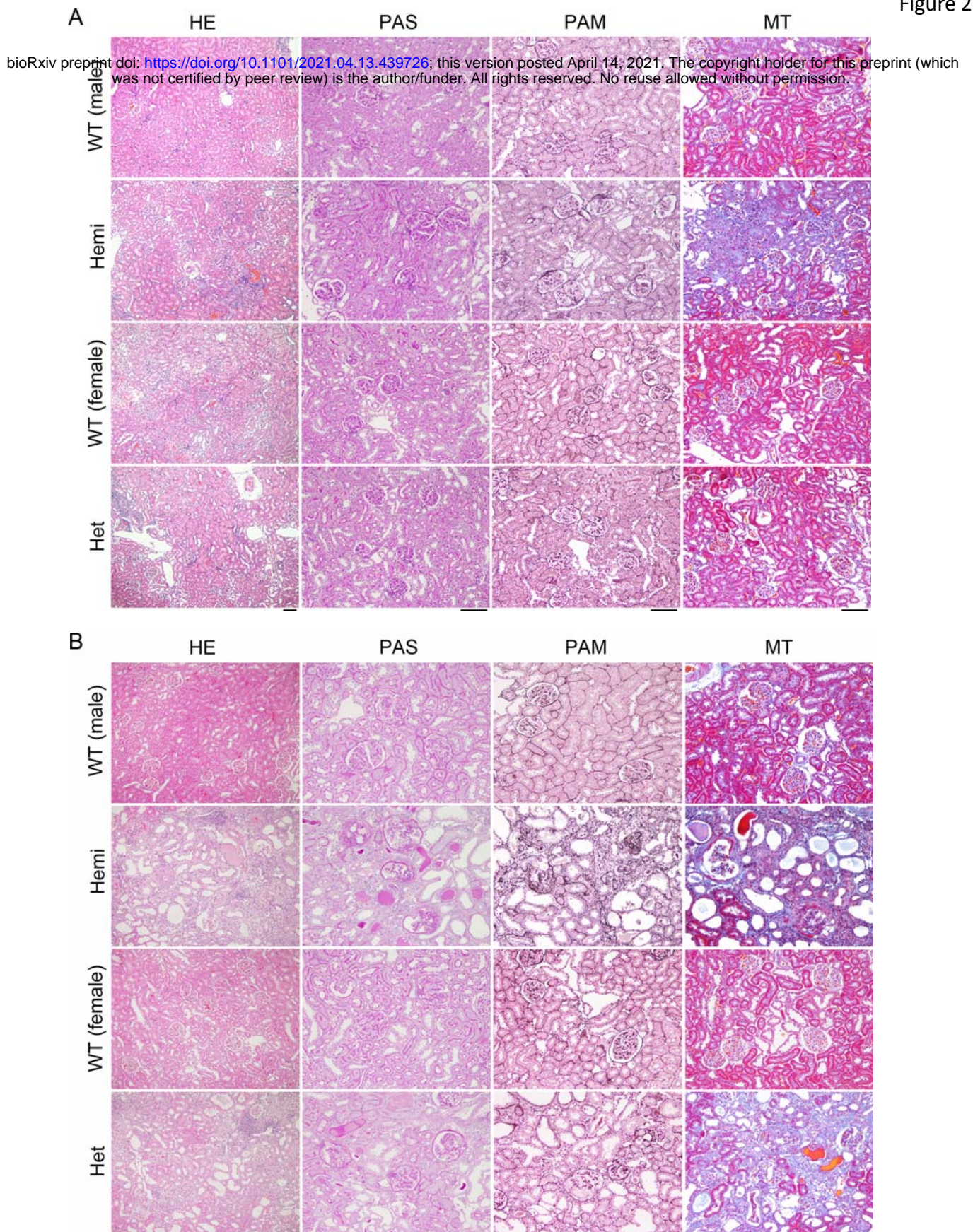
20. Sado Y, Boutaud A, Kagawa M, Naito I, Ninomiya Y, Hudson BG: Induction of anti-GBM nephritis in rats by recombinant alpha 3(IV)NC1 and alpha 4(IV)NC1 of type IV collagen. *Kidney Int*, 53: 664-671, 1998 10.1046/j.1523-1755.1998.00795.x S0085-2538(15)60442-2 [pii]
21. Aitman TJ, Dong R, Vyse TJ, Norsworthy PJ, Johnson MD, Smith J, et al.: Copy number polymorphism in *Fcgr3* predisposes to glomerulonephritis in rats and humans. *Nature*, 439: 851-855, 2006 nature04489 [pii] 10.1038/nature04489
22. Meek S, Mashimo T, Burdon T: From engineering to editing the rat genome. *Mamm Genome*, 28: 302-314, 2017 10.1007/s00335-017-9705-8 10.1007/s00335-017-9705-8 [pii]
23. Szpirer C: Rat models of human diseases and related phenotypes: a systematic inventory of the causative genes. *J Biomed Sci*, 27: 84, 2020 10.1186/s12929-020-00673-8
24. Takahashi G, Gurumurthy CB, Wada K, Miura H, Sato M, Ohtsuka M: GONAD: Genome-editing via Oviductal Nucleic Acids Delivery system: a novel microinjection independent genome engineering method in mice. *Sci Rep*, 5: 11406, 2015 10.1038/srep11406 srep11406 [pii]
25. Ohtsuka M, Sato M, Miura H, Takabayashi S, Matsuyama M, Koyano T, et al.: i-GONAD: a robust method for in situ germline genome engineering using CRISPR nucleases. *Genome Biol*, 19: 25, 2018 10.1186/s13059-018-1400-x
26. Kobayashi T, Namba M, Koyano T, Fukushima M, Sato M, Ohtsuka M, et al.: Successful production of genome-edited rats by the rGONAD method. *BMC Biotechnol*, 18:19, 2018 10.1186/s12896-018-0430-5
27. Gurumurthy CB, Sato M, Nakamura A, Inui M, Kawano N, Islam MA, et al.: Creation of CRISPR-based germline-genome-engineered mice without ex vivo handling of zygotes by i-GONAD. *Nat Protoc*, 14: 2452-2482, 2019 10.1038/s41596-019-0187-x
28. Ninichuk V, Gross O, Reichel C, Khandoga A, Pawar RD, Ciubar R, et al.: Delayed chemokine receptor 1 blockade prolongs survival in collagen 4A3-deficient mice with Alport disease. *J Am Soc Nephrol*, 16: 977-985, 2005 10.1681/ASN.2004100871
29. Koepke ML, Weber M, Schulze-Lohoff E, Beirowski B, Segerer S, Gross

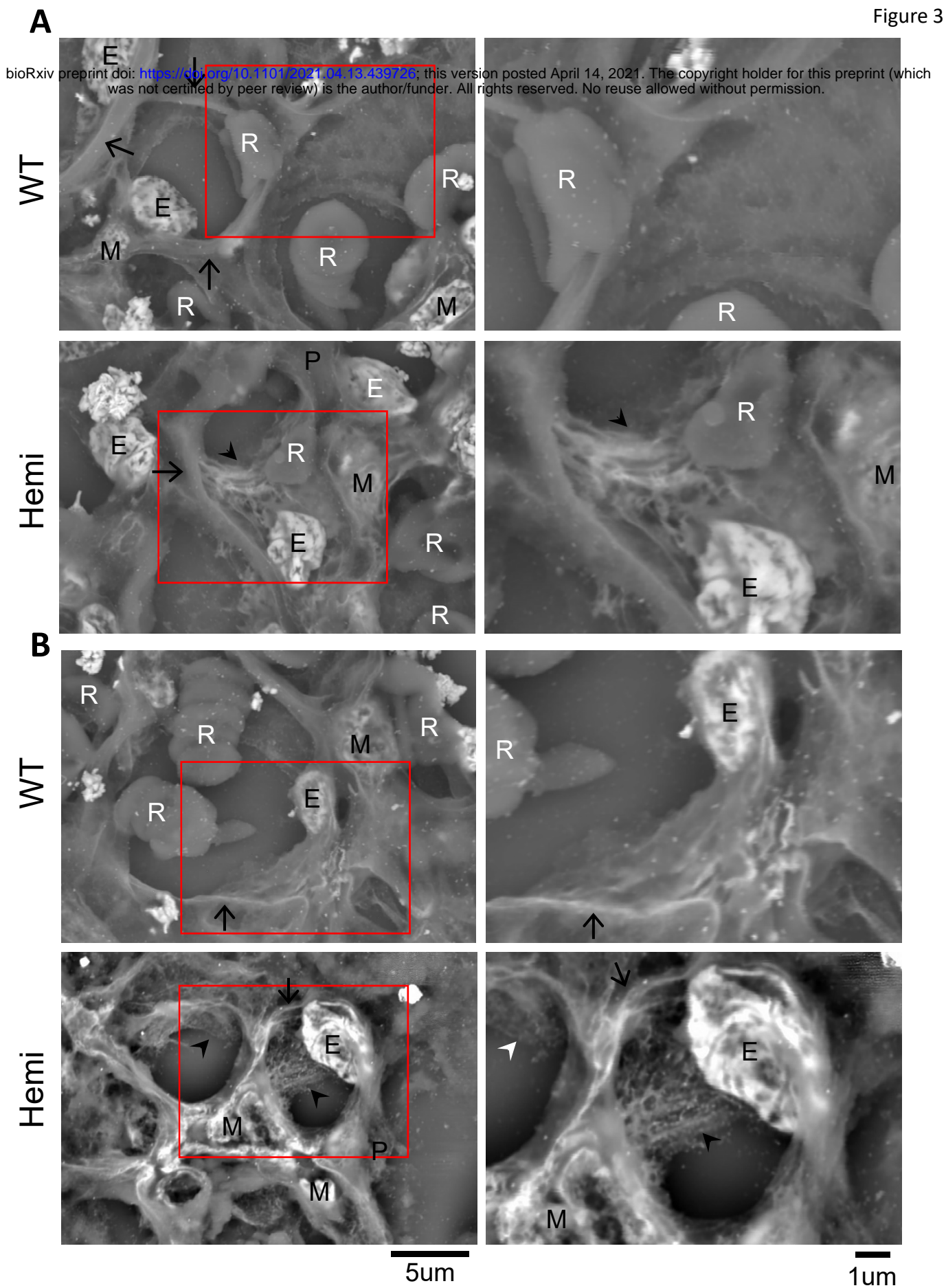
- 0: Nephroprotective effect of the HMG-CoA-reductase inhibitor cerivastatin in a mouse model of progressive renal fibrosis in Alport syndrome. *Nephrol Dial Transplant*, 22: 1062–1069, 2007 10.1093/ndt/gf1810
30. Cosgrove D, Dufek B, Meehan DT, Delimont D, Hartnett M, Samuelson G, et al.: Lysyl oxidase like-2 contributes to renal fibrosis in Col4alpha3/Alport mice. *Kidney Int*, 94: 303–314, 2018 10.1016/j.kint.2018.02.024
31. Omachi K, Kaseda S, Yokota T, Kamura M, Teramoto K, Kuwazuru J, et al.: Metformin ameliorates the severity of experimental Alport syndrome. *Sci Rep*, 11: 7053, 2021 10.1038/s41598-021-86109-1
32. Andrews KL, Mudd JL, Li C, Miner JH: Quantitative trait loci influence renal disease progression in a mouse model of Alport syndrome. *Am J Pathol*, 160: 721–730, 2002 10.1016/S0002-9440(10)64892-4
33. Gross O, Borza DB, Anders HJ, Licht C, Weber M, Segerer S, et al.: Stem cell therapy for Alport syndrome: the hope beyond the hype. *Nephrol Dial Transplant*, 24: 731–734, 2009 10.1093/ndt/gfn722
34. Gross O, Beirowski B, Koepke ML, Kuck J, Reiner M, Addicks K, et al.: Preemptive ramipril therapy delays renal failure and reduces renal fibrosis in COL4A3-knockout mice with Alport syndrome. *Kidney Int*, 63: 438–446, 2003 10.1046/j.1523-1755.2003.00779.x
35. Smith JR, Bolton ER, Dwinell MR: The Rat: A Model Used in Biomedical Research. *Methods Mol Biol*, 2018: 1–41, 2019 10.1007/978-1-4939-9581-3_1
36. Jacob HJ: The rat: a model used in biomedical research. *Methods Mol Biol*, 597: 1–11, 2010 10.1007/978-1-60327-389-3_1
37. Aitman T, Dhillon P, Geurts AM: A RAtional choice for translational research? *Dis Model Mech*, 9: 1069–1072, 2016 10.1242/dmm.027706
38. Hunziker MH, Saldana RL, Neuringer A: Behavioral variability in SHR and WKY rats as a function of rearing environment and reinforcement contingency. *J Exp Anal Behav*, 65: 129–144, 1996 10.1901/jeab.1996.65-129
39. Matsuyama M, Nomori A, Nakakuni K, Shimono A, Fukushima M: Secreted Frizzled-related protein 1 (Sfrp1) regulates the progression of renal fibrosis in a mouse model of obstructive nephropathy. *J Biol Chem*, 289: 31526–31533, 2014 10.1074/jbc.M114.584565

M114.584565 [pii]

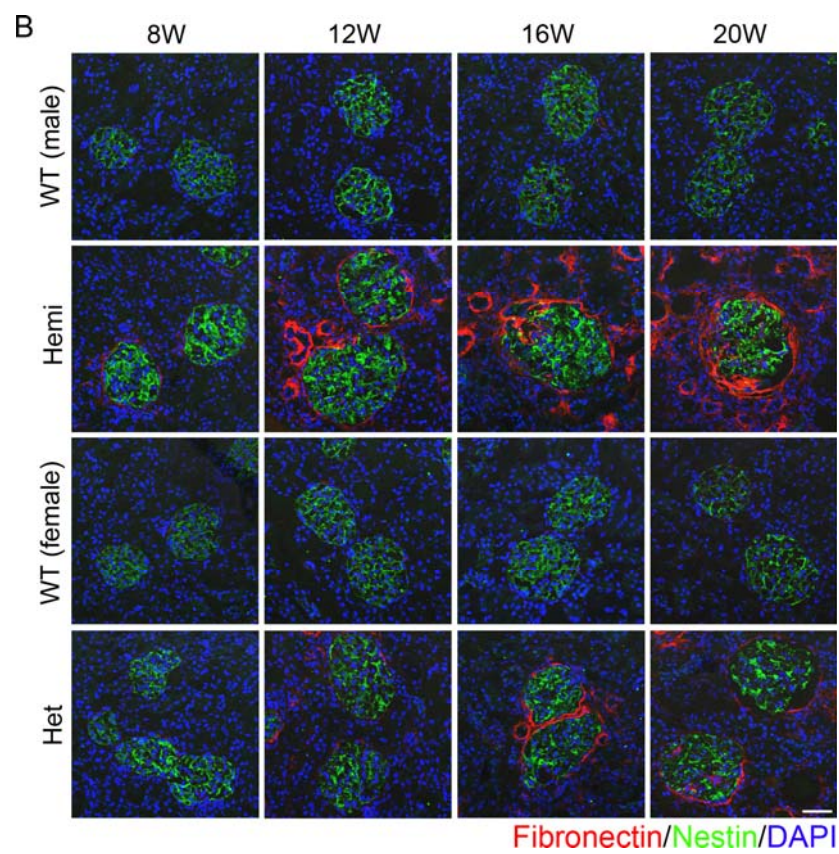
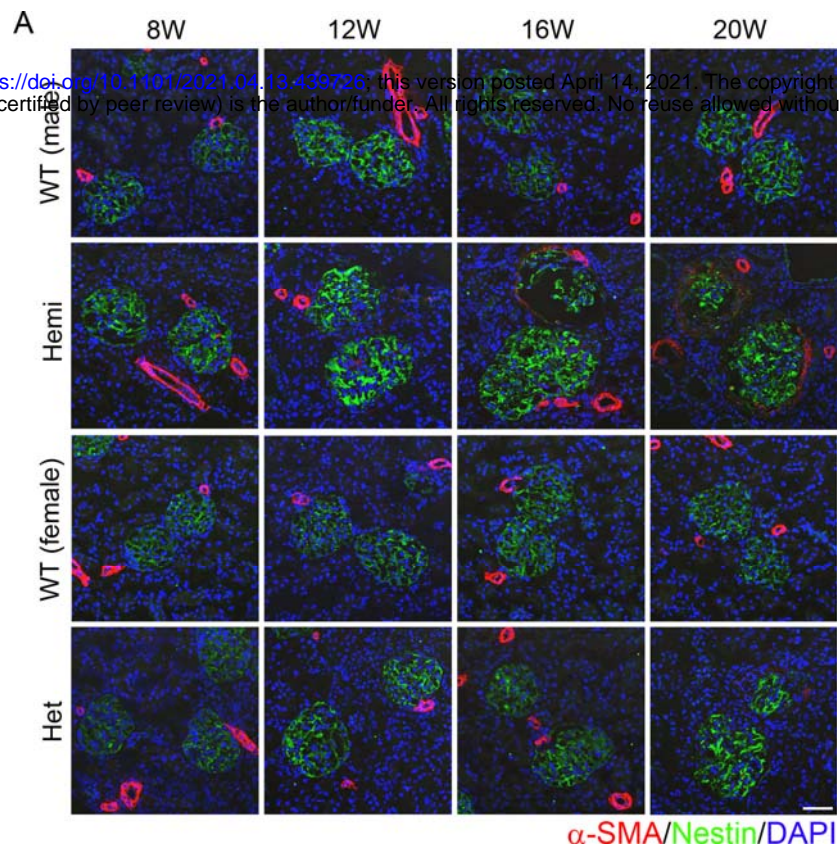
40. Okada S, Inaga S, Kitamoto K, Kawaba Y, Nakane H, Naguro T, et al.: Morphological diagnosis of Alport syndrome and thin basement membrane nephropathy by low vacuum scanning electron microscopy. *Biomed Res*, 35: 345-350, 2014 10.2220/biomedres.35.345
41. Kishiro Y, Kagawa M, Naito I, Sado Y: A novel method of preparing rat-monoclonal antibody-producing hybridomas by using rat medial iliac lymph node cells. *Cell Struct Funct*, 20: 151-156, 1995 10.1247/csf.20.151
42. Sado Y, Inoue S, Tomono Y, Omori H: Lymphocytes from enlarged iliac lymph nodes as fusion partners for the production of monoclonal antibodies after a single tail base immunization attempt. *Acta Histochem Cytochem*, 39: 89-94, 2006 10.1267/ahc.06001
43. Ninomiya Y, Kagawa M, Iyama K, Naito I, Kishiro Y, Seyer JM, et al.: Differential expression of two basement membrane collagen genes, COL4A6 and COL4A5, demonstrated by immunofluorescence staining using peptide-specific monoclonal antibodies. *J Cell Biol*, 130: 1219-1229, 1995 10.1083/jcb.130.5.1219
44. Matsuyama M, Tanaka H, Inoko A, Goto H, Yonemura S, Kobori K, et al.: Defect of mitotic vimentin phosphorylation causes microphthalmia and cataract via aneuploidy and senescence in lens epithelial cells. *J Biol Chem*, 288: 35626-35635, 2013 10.1074/jbc.M113.514737
45. Koyano T, Namba M, Kobayashi T, Nakakuni K, Nakano D, Fukushima M, et al.: The p21 dependent G2 arrest of the cell cycle in epithelial tubular cells links to the early stage of renal fibrosis. *Sci Rep*, 9: 12059, 2019 10.1038/s41598-019-48557-8





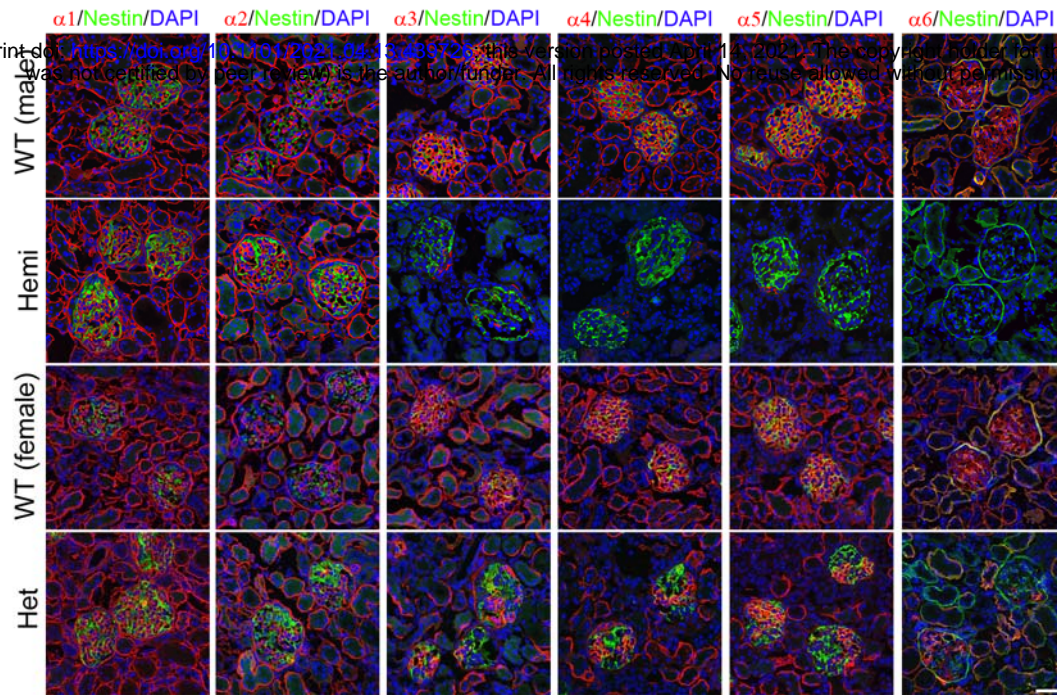


bioRxiv preprint doi: <https://doi.org/10.1101/2021.04.13.439726>; this version posted April 14, 2021. The copyright holder for this preprint (which was not certified by peer review) is the author/funder. All rights reserved. No reuse allowed without permission.

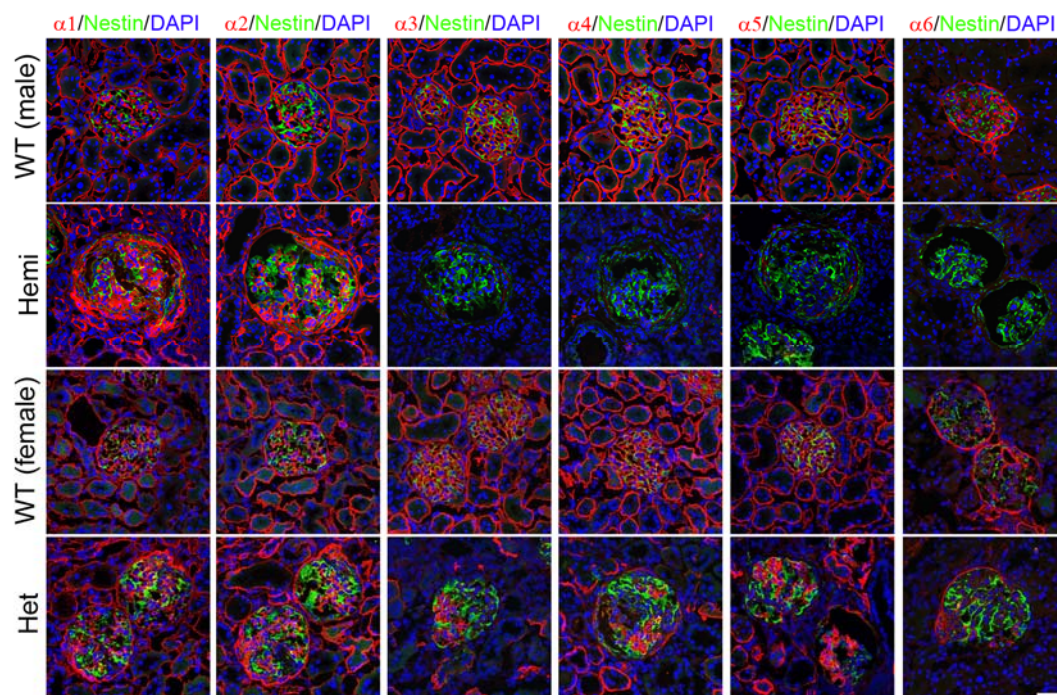


A

bioRxiv preprint doi: <https://doi.org/10.1101/2021.04.15.437278>; this version posted April 15, 2021. The copyright holder for this preprint (which was not certified by peer review) is the author/funder. All rights reserved. No reuse allowed without permission.



B



bioRxiv preprint doi: <https://doi.org/10.1101/2021.04.13.439726>; this version posted April 14, 2021. The copyright holder for this preprint (which was not certified by peer review) is the author/funder. All rights reserved. No reuse allowed without permission.

